Carleton Geology Department

Geology Comps Papers

Carleton College *Year* 2004

Determining the source for the magmas of Monte Amiata (Central Italy) using strontium, neodymium, and lead isotopes

Kristen James

Determining the Source for the Magmas of Monte Amiata (Central Italy) Using Strontium, Neodymium, and Lead Isotope Analysis

Kristen James
Carleton College Senior Integrative Exercise
March 10, 2004

Bereket Haileab: Advisor

Submitted in partial fulfillment of the requirements for a Bachelor of Arts degree from Carleton College, Northfield, Minnesota

Table of Contents

Determining the Source for the Magmas of Monte Amiata (Central Italy) Using Strontium, Neodymium, and Lead Isotope Analysis

Kristen James

Carleton College Senior Integrative Exercise
March 10, 2004

Bereket Haileab: Advisor

Abstract

Monte Amiata is a recently extinct volcano that produced trachydacites and a few small olivine latite flows. The Amiata suite showed crustal strontium, neodymium, and lead isotopic signatures. $^{87}Sr/^{86}Sr$ ratio values ranged from 0.712447 to 0.713068 and $^{143}Nd/^{144}Nd$ ratios ranged from 0.512094 to 0.512203. $^{207}Pb/^{204}Pb$ values ranged from 15.6694 to 16.2330 and $^{206}Pb/^{204}Pb$ ratios ranged from 18.7125 to 19.0882. The olivine latite flows towards the end of volcanic activity would suggest more mantle influence than the data suggests, but Amiata may be sourcing from a depleted mantle as well as the limestone that proliferates throughout Italy. Strontium concentrations are similar to those of rubidium, so neodymium-samarium comparisons were utilized, as they are more reliable. Neodymium concentrations, when placed against samarium concentrations, indicate crustal contamination, as do the isotope data.

Keywords: strontium, neodymium, lead, isotopes, TMP, RMP

Introduction

The western edge of the Italian peninsula is a complicated geologic setting, both tectonically and geochemically. The volcanoes that cover the western edge of the peninsula from northern Tuscany to south of Rome are divided into two distinct magmatic provinces (Figure 1), the northern Tuscan Magmatic Province (TMP) and the southern Roman Magmatic Province (RMP). One of the volcanoes that lie on the TMP/RMP boundary is Monte Amiata (Figure 2), a young volcano that was active from approximately 300-200 ka (Ferrari, 1996). Samples were taken from six units: the Basal Trachydacite unit (upper and lower), the Poggio Lombardo unit, the Poggio Biello unit, the La Vetta unit, and the Pianello unit.

TMP magmas are more silica rich than RMP magmas due to partial melting of the metasedimentary limestones throughout Italy (Giraud, 1986). Amiata produces trachydacites that are slightly silica undersaturated to oversaturated with plagioclase clinopyroxene, sanidine, and olivine as the main phenocryst phases. They often have relatively high SiO_2 levels, as well as high K_2O, MgO, and Ni abundances (Conticelli, 2002; Poli, 1984).

Van Bergen (1983) first hypothesized that the origin for Amiata magmas was a mixing between the TMP and RMP magmas. Within a year of this conjecture, isotope work done on Amiata and surrounding volcanoes showed that the Amiata rocks are more likely the product of mixing processes between a high-K series of the RMP and silicic crustal components (Poli, 1984). If simple two component mixing is assumed, it must mean that the two end members are nearly equally rich in Rb, Zr, La, Ce, Nb, and Y or that the absence of variation is due to a homogenization process that took place in the

magma chamber (Van Bergen, 1985). A study involving Amiata, Roccastrada, and San Vicenzo furthered the theory of equal end-member concentrations and showed an evolutionary trend of decreasing concentration of Ba, Sr, Ti, V, Zr, Hf, Pb and LREE from Amiata, with the lowest silica content, to Roccastrada, with the highest silica content (Giraud, 1986). Chemistry of the mantle generated end-member indicated that crustally contaminated asthenosphere began melting 0.6 Ma to produce the undersaturated mantle derived end-member of the Monte Amiata mixing line and that this process must have involved a boundary layer and crustal rocks (Ferrari, 1996). Also, the concentration of radiogenic elements (mainly Nd) in these rocks would indicate a great amount of crustal contamination and may also affect major and trace element concentrations in these magmas (Castorina, 2000).

This paper will show that mixing between RMP and crustal material is the most likely source for the magmas at Amiata. Also, it will argue that, because samples ratios plot near marine sediment values for both $^{87}Sr/^{86}Sr$ and $^{143}Nd/^{144}Nd$, recycled marine sediments are a probable source of crustal contamination in the asthenosphere.

I will present my findings in three stages. First, I will present major and trace element analyses of the lavas and explain the chemical content of the Amiata suite. Second, I will analyze the lead, strontium, and neodymium isotope data that I obtained. And finally, I will discuss the accuracy of my hypothesis in relation to all of the data.

Geologic Setting

Approximately 15 Ma, the Tyrrhenian Sea began to open along a North-South rift that parallels the eastern edge of Corsica-Sardinia (Lavecchia, 1990). The Tyrrhenian

eastern peninsular margin consists of NW-SE, NW-SSE sets of grabens bounded by westward-dipping faults. Throughout Tuscany and Calabria low- and high-angle extensional features proliferated while this region followed a delamination model for lithospheric extension, with basal detachment caused by shallow, low-angle normal faulting (Lavecchia, 1987; Lavecchia, 1990, 1996).

During the Neogene and into the Quaternary the region around Amiata underwent a general NNE contraction (Lavecchia, 1987). This created splay thrusts that pushed up and shortened both basement rocks and cover sedimentary rocks in the region (Lavecchia, 1987). This compression also created the Apennine orogeny of east-central Italy. The TMP, has been magmatically active since the middle Miocene, but Amiata is on the tail end of that magmatic activity (Lavecchia, 1987; Lavecchia, 1990, 1996).

Subsequent post-orogenic (Apennine orogeny) normal faulting led to the formation of several NNW-SSE horst and graben systems (Ferrari, 1996). Amiata sits on the western side of the Siena-Radicofani basin, which was filled with more than 1000 meters of marine sediments (Ferrari, 1996). This area was brought above sea level during a regional doming phase during the Middle Pliocene. Uplift of the Amiata region occurs along an ENE-WSW direction (Ferrari, 1996).

A low-density, seismically transparent body at a depth of about 6-7 km below Monte Amiata is believed to be broader than the volcano and the known geothermal field in the area (Volpi, 2003). This body is probably cooling magma, still partially molten, that deepens and then disappears beyond the volcanic edifice (Volpi, 2003).

Methods

Twenty-six samples were collected from around Monte Amiata in southern Tuscany, Italy. Four samples were used to make thin sections during the preliminary phases of this project to determine general mineral content of the Basal Trachydacite Complex, upper and lower units, the La Vetta unit, and the Poggio Biello unit. Of the original twenty-six, twelve samples were chosen using location and quality of the sample as parameters. Isotope, major, and trace element analyses were performed on these samples. Isotope analysis was performed at the Carnegie Institution of Washington under the supervision of Drs. Rick Carlson and Steve Shirey. Major and trace element analyses were done at the Washington State University GeoAnalytical Lab.

Strontium, neodymium, and lead isotope analysis was performed using resin column separation chemistry and mass spectrometry. These samples were rough crushed using a rock hammer, then further crushed to uniform sand-sized particles using a jaw crusher. The sand-sized particles were then crushed to a homogenous powder in an aluminum shatterbox. Approximately 100 mg of sample was measured out and dissolved in a 2:1 ratio of concentrated HF acid and 16 N HNO_3 for one hour, uncapped, on a hotplate with a heat lamp directly above. They were then capped and left on the hotplate for one day. Once the samples had been fully dissolved, they were evaporated to dryness and 1mL of HNO_3 was added and the sample dried. This step was repeated a second time, after which approximately 2mL of 4N HCl was added. The sample was evaporated to dryness one last time and then prepped for lead column chemistry by dissolving the sample in ~1mL of 0.5N HBr, drying down slowly and then adding ~3mL of HBr (Geochemistry Group, 2003a).

The columns for lead separation were prepared and then cleaned with 6mL 8N HNO_3 and then another 6mL of 0.5N HNO_3. 0.5mL of MilliQ (MQ) water was added to remove the NO_3^-. Next, 0.5mL of 0.5N HBr was added to charge the resin with Br^- anions, after which the 3mL of sample was added. HBr was eluted in three stages after the sample was loaded, 0.3mL, 0.5mL, and 0.5mL. 1mL of HNO_3 was run through the column to remove lead from the resin. This cut was collected and the column was then cleaned with 6mL 0.5N HNO_3, 0.5mL MQ, and prepped with 0.5mL HBr. The lead cut was added and HBr was eluted in two 0.5mL runs to remove remaining cations, after which 1mL of HNO_3 was added to remove the lead. One drop of phosphoric acid was added to the collected sample before drying so the sample could be easily found once dried down (Geochemistry Group, 2003a).

Primary separation columns were run next to separate hafnium, strontium, and neodymium. The samples, after running lead columns, were dried down and redissolved in the HF-HNO_3 mixture. Two HNO_3 drydowns were done at which point samples were redissolved in 1-2N HCl and then dried. They were then prepped for columns by dissolving them in 5mL 0.1N HF-1N HCl. The columns were conditioned with 20mL of 0.1N HF-1N HCl and then the 5mL of sample were added. This fraction was collected immediately for the hafnium cut, as was the following 5mL of 0.1N HF-1N HCl. Next 30mL of 2.5N HCl was eluted. 14mL of 2.5N HCl was collected for the strontium fraction, which was dried down and left until mass spectrometry was performed. 12mL of 4N HCl was eluted and the last step was to collect 16mL of 4N HCl for the Nd-Sm fraction. Columns were then cleaned with 1 full reservoir of 6N HCl and sample cuts were dried down (Geochemistry Group, 2003a).

Neodymium separation columns were prepared and the samples were prepped for the run by placing one drop of 0.1N HCl on the dry sample. After the resin had been added to the columns, one drop of MQ water was added and air bubbles removed. Samples were added directly into the luer tip of the column, with one more drop of MQ added on top of it. At this point Methyllactic Acid (MLA) was added to the top of the column junction and the syringe body was inserted into the luer tip. 10mL of MLA was added to the syringe body, the tops were stoppered and N_2 gas was run through. From the 4-1.2mL reading on the syringe body, the Nd fraction was collected (Geochemistry Group, 2003a).

Pb samples were loaded onto a Re filament in 1N HNO_3. The filament had1μ of Silica-gel and 1% H_3PO_4 loaded onto it before loading the lead sample. The filaments were heated up to approximately 1 amp (around 80ºC) until dry and then taken to a dull red color and slowly cooled. Sr was also loaded on Re filaments, but these filaments had a Ta_2O_5 film loaded onto them first. The Sr was loaded in 1N HNO_3, dried at 1 amp, heated to a dull red for 5 counts and then cooled slowly. Lead and strontium were both run on a VG 350 mass spectrometer. There was a great deal of trouble with the lead samples burning off due to pyrometer malfunction.

Nd was loaded in 1N HNO_3 run on an ICP 54 using different dilutions (usually 4:1) that would allow the machine to run at between 2 and 5 volts. Samples were self-aspirated into a CETAC MCN-6000 Desolvating Nebulizer and, from there, into the torch of the ICP. Data was put into spreadsheets provided by Carnegie that took into account the fractionation of the isotopes and produced corrected values. These are the values used in all figures (Geochemistry Group, 2003b).

Major elements were determined using XRF and trace elements by ICP-MS (Johnson, 1999; Knaack, 1994). Data had been normalized by the technicians at the WSU GeoAnalytical Lab and were ready to be plotted when received by the author.

Results

Thin Sections:

All samples contained quartz, plagioclase, clinopyroxene, biotite, and some iron or titanium oxides. The matrix of each rock was made up of extremely small quartz, plagioclase, and glass shards. The plagioclase showed a distinct oscillatory zoning.

Major and trace elements:

The trachydacites of Monte Amiata are extremely silica-rich, ranging from 62.06 to 67.43 wt.% SiO_2. Potassium levels were relatively high, ranging from 5.55 to 6.19 wt.% K_2O. Na_2O levels ranged from 1.98 to 2.37 wt.%. MgO levels were overall very low, ranging from 1.34 to 1.78, with only sample 19 outside of these bounds at 2.73 wt.%. The same pattern holds true for FeO and MnO, with ranges from 3.33 to 3.97 wt.% and 0.058 to 0.070 wt.% with sample 19 at 4.70 wt.%, and 0.081 wt.%, respectively. TiO_2 levels were low, ranging from 0.516 to 0.677 wt.%. Al_2O_3 levels ranged from 16.17 to 17.78 wt.%, and P_2O_5 levels ranged from 0.164 to 0.197 wt.%, with sample 19 again falling outside of the range at 0.243 wt.%. CaO levels were surprisingly low, ranging from 2.64 to 3.06, and sample 19 at 4.5 wt.% (Table 1).

Trace element data (Table 2) was very tight, with all elements having similar concentrations. Figure 4 shows a low europium anomaly, with 1.38-1.83 ppm. Heavier REE had higher overall concentrations, with La values ranged from 67.06-83.80 ppm, Ce

values ranged from 126.71-143.72 ppm, and Pr values ranging from 13.77-17.11 ppm. Lighter REE had lower concentrations, with Tm ranging from 0.41-0.47 ppm, Yb ranging from 2.50-2.90 ppm, and Lu ranging from 0.39-0.46 ppm (Figure 4). Y values range from 28.91 to 36.35 ppm, Zr from 214-246 ppm, and Nb from 16.69-20.0 ppm (Figure 5). Nd levels range from 51.22-63.76, with Sm concentrations ranging from 10.04-12.61 ppm (Figure 6). There were similar levels of strontium, 327-451ppm, and rubidium, 308-382 ppm (Figure 7). Pb values ranged from 57.83-63.24 ppm and U levels ranged from 10.07-11.40 ppm. Ba had a high concentration, ranging from 431-676 ppm, as did Th, which ranged from 41.4-49.8 ppm. Cs ranged from 20.89-45.58 ppm, and Sc ranged from 10.3-17.0 ppm. Gd levels ranged from 7.24-9.24 and Hf levels ranged from 6.58-7.98 ppm. Dy ranges from 5.73-6.99 ppm and Er from 2.87-3.33 ppm. Ta ranged from 1.49-1.92 with an anomalous high value of 5.63 ppm for sample 12. Ho ranges from 1.09-1.31 ppm, and Tb ranged from 1.04-1.30 ppm.

Stable Isotope Results

$^{87}Sr/^{86}Sr$ ratios range from 0.712447 to 0.713068. $^{143}Nd/^{144}Nd$ values range from 0.512094 to 0.512203. $^{206}Pb/^{204}Pb$ ratio values range from 18.7125 to 19.0882. $^{207}Pb/^{204}Pb$ values range from 15.6694 to 16.2330 (Table 3).

Discussion

Thin Sections:

Mineralogy of the Amiata suite (as determined from thin sections) was almost identical to that already described in detail by previous studies (Conticelli, 2002; Poli, 1984). The oscillatory zoning of the plagioclase crystals could imply a static condition in

the magma chamber (Lux, 2003), which would further the theory that Amiata sourced from the same types of rocks throughout its eruption history.

Major and trace elements:

The data plots clearly in the trachydacite field, except for one, which plots in the trachyandesite field on the Total alkali vs. silica (TAS) diagram (Figure 3). These rocks are hypersthene and quartz normative and plagioclase and pyroxenes dominate as the main phenocryst phases (Poli, 1984). Of the trace elements, the REEs were chondrite normalized and plotted (Figure 4). The europium anomaly is most likely indicative of plagioclase fractionation in the magma chamber (Rollinson, 1993). It is also possible, since there appears to be an enrichment of lighter REEs, that hornblende could have been present in the samples (Rollinson, 1993), but not identified in thin section because it was part of the matrix. In Figure 5, Y was plotted against Zr in one plot, and against Nb in the second plot. Should either of these graphs have shown two distinct clusters of points, bimodal volcanism could have been assumed. However, as neither shows this trend, we can be sure that our previous assumption of a single magma chamber was accurate. Also, these clusters are so compact that it is clear that the Amiata suite was sourcing from the same rocks, at a set depth during the entire time of magma generation. Although these plots are normally used for basalts, and we are dealing with dacites, this interpretation is still sound.

Nd values (Table 2) show a greater amount of radiogenic Nd than Sm, indicating a crustal source for the dacites (Figure 6). Sr and Rb have similar concentrations (Figure7). Sr concentrations are slightly lower than Rb in all but samples 13, 17, and 19, when Rb concentrations are slightly lower than Sr (Table 2). The Sr concentrations are

on the lower end of the spectrum of volcanoes in western Italy. Sr concentrations can range up to ~1500 ppm (Conticelli, 2002). In the vast majority of these samples, Sr concentrations are usually 1.5 or 2 times higher than Rb concentrations (Conticelli, 2002). Also, Sr concentrations in marine sediments can range greatly, from ~100-900 ppm (Othman, 1989), and in the Aeolian Arc, Sr concentrations are greater than Rb concentrations by orders of magnitude (Esperanca, 1992; Francalanci, 1993). Sr and Rb are relatively mobile elements, and therefore the Nd-Sm concentrations are more robust indicators of source (Rollinson, 1993). Also, because there is such a high concentration of both Sr and Rb, isotopic Sr ratio levels may not be reliable at all (Table 2).

Stable Isotopes:

All the isotopic data suggests a crustal source. When the $^{143}Nd/^{144}Nd$ values are plotted against $^{87}Sr/^{86}Sr$, all samples fall in the lower right quadrant, which is indicates a crustal source from both the Sr and Nd ratio values (Figure 8). More importantly, the Sr isotope ratios, as stated above, may not be reliable due to the Sr-Rb concentration similarities in the samples. The high $^{87}Sr/^{86}Sr$ ratios could be due to the strontium anomaly in the mantle from eastern Italy (Stoppa, 2003), or they could be as high as they are simply because there is an abundance of strontium in the crustal rocks of the area. Also, if the mantle source were undersaturated, as suggested by (Ferrari, 1996) then Rb levels could be lower than usual, and with such a high concentration of Sr, it would be logical to assume a crustal anatectic source for these rocks. $^{87}Sr/^{86}Sr$ levels, when plotted against $^{206}Pb/^{204}Pb$, fall well into the crustal area (Figure 9).

The Nd values are more reliable because there is more Nd than Sm in the samples, indicating a crustal source, as well as the $^{143}Nd/^{144}Nd$ values, which fall distinctly into the

crustal field when plotted (Figure 10). Both the $^{143}Nd/^{144}Nd$ and $^{87}Sr/^{86}Sr$ values, when plotted against $^{206}Pb/^{204}Pb$ values plot very close to the marine sediments field, indicating that recycled marine sediments probably contributed a great deal of material to the magmas of Amiata (Figures 9 and 10).

There are three anomalously high $^{207}Pb/^{204}Pb$ ratio values that, when plotted against $^{206}Pb/^{204}Pb$ values plot a great deal higher than any of the other fields (Figure 11). However, considering that the remaining values plot near the marine sediment field, it can be assumed that the previous assumption from the Sr and Nd ratios holds true.

Conclusions

The samples from Monte Amiata are all geochemically and isotopically similar. From the data, it can be inferred that Amiata sourced from one type of crustal rock (most likely limestone) and an undersaturated mantle source. Marine sediments from the subducting plate under western Italy as well as the 1000 meters of marine sediments deposited in the Radicofani graben to the east provided a great deal of material that went into the melt at Amiata. Crustal anatexis is the most likely explanation for volcanism at Amiata, which is further proven by the shallow geothermal field that exists under the area. Crustal contamination may have been prolific considering the amount of Nd as compared to Sm found in the samples, and therefore we can say that the hypothesis that RMP and crustal rocks were the source for this volcano (Van Bergen, 1985) is accurate and be able to add that marine sediments may have played a large role in the volcanism at Amiata.

Acknowledgments

I would like to acknowledge Dr. Francesco Stoppa for helping me formulate the idea for this project, as well as Drs. Rick Carlson and Steve Shirey, and the Carnegie technicians for their unending patience and wonderful help during the data-gathering phase. Special thanks go to Bereket Haileab for his encouragement and constructive criticisms. I could not have done this without him. I would also like to thank those who have donated to the Carleton College Geology Department for making this work possible. Special thanks go to Jeremy Hoehn and David Hendler, whose help trouble-shooting my multitude of computer problems was invaluable. To my family, I am grateful for your support. So thanks. Tim Vick, you are my co-pilot. And finally, to the staff of Perkins: thanks for keeping the coffee coming. You fantastic people have allowed me to sit down and get this done, and I thank you all.

References:

Caprarelli, G. T., Shigeko; De Vivo, Benedetto, 1993, Preliminary Sr and Nd isotopic data for recent lavas from Vesuvius volcano.: Journal of Volcanology and Geothermal Research, v. 58, p. 377-381.

Castorina, F. S., F.; Cundari, A.; Barbieri, M., 2000, An enriched mantle source for Italy's melilite-carbonatite association as inferred by its εNd-Sr isotope signature: Mineralogical Magazine, v. 64, no. 4, p. 155-169.

Civetta, L. G., Gabriella; Orsi, Giovanni, 1991, Sr- and Nd-isotope and trace-element constraints on the chemical evolution of the magmatic system of Ischia (Italy) in the last 55 ka.: Journal of Volcanology and Geothermal Research, v. 46, p. 213-230.

Conticelli, S., D'Antonio, M., Pinarelli, L., Civetta L., 2002, Source contamination and mantle heterogeneity in the genesis of Italian potassic and ultrapotassic volcanic rocks: Sr-Nd-Pb isotope data from Roman Province and Southern Tuscany: Mineralogy and Petrology, v. 74, p. 189-222.

Conticelli, S. F., L.; Santo, A.P., 1991, Petrology of final-stage Latera lavas (Vulsini Mts.): mineralogical, geochemical and Sr-isotopic data and their bearing on the genesis of some potassic magmas in central Italy.: Journal of Volcanology and Geothermal Research, v. 46, p. 187-212.

Conticelli, S. F., Lorella; Manetti, Piero; Cioni, Raffaello; Sbrana, Alessandro, 1997, Petrology and geochemistry of the ultrapotassic rocks from the Sabatini Volcanic District, central Italy: the role of evolutionary processes in the genesis of variably enriched alkaline magmas.: Journal of Volcanology and Geothermal Research, v. 75, p. 107-136.

Ellam, R. M. H., C.J.; Menzies, M.A.; Rogers, N.W., 1989, The volcanism of southern Italy: Role of subduction and the relationship between potassic and sodic alkaline magmatism.: Journal of Geophysical Research, v. 94, no. B4, p. 4589-4601.

Esperanca, S. C., G.M.; de Rosa, R.; Mazzuoli, R., 1992, The role of the crust in the magmatic evolution of the island of Lipari (Aeolian Islands, Italy). Contributions to Mineralogy and Petrology, v. 112, p. 450-462.

Ferrara, G. P., R.; Serri, G.; Tonarini, S., 1989, Petrology and isotope-geochemistry of San Vicenzo rhyolites (Tuscany, Italy). Bulletin of Volcanology, v. 51, p. 379-388.

Ferrari, L. C., S.; Burlamacchi, L.; Manetti, P., 1996, Volcanological evolution of the Monte Amiata, Southern Tuscany: New geological and petrochemical data: Acta Vulcanologica, v. 8, no. 1, p. 41-56.

Francalanci, L. T., S.R.; McCulloch, M.T.; Woodhead, J.D., 1993, Geochemical and isotopic variations in the calc-alkaline rocks of Aeolian arc, southern Tyrrhenian Sea, Italy: constraints on magma genesis.: Contributions to Mineralogy and Petrology, v. 113, p. 300-313.

Geochemistry Group, D. o. T. M., 2003a, Laboratory Instructions for Column Chemistry, *in* James, K., ed.: Washington, D.C.

Geochemistry Group, D. o. T. M., 2003b, Mass Spectrometry Fractionation Correction Spreadsheets, *in* James, K., ed.: Washington, D.C.

Giraud, A., Dupuy, C., Dostal, J., 1986, Behavior of trace elements during magmatic processes in the crust: application to acidic volcanic rocks of Tuscany (Italy). Chemical Geology, v. 57, p. 269-288.

Hawkesworth, C. J. V., R., 1979, Crustal contamination versus enriched mantle: 143Nd/144Nd and 87Sr/86Sr evidence from the Italian volcanics.: Contributions to Mineralogy and Petrology, v. 69, p. 151-165.

Holm, P. M. M., Niels Crosley, 1982, Evidence for mantle metasomatism: an oxygen and strontium isotope study of the Vulsinian District, Central Italy.: Earth and Planetary Science Letters, v. 60, p. 376-388.

Ito, E. W., William M.; Gopel, Christa, 1987, The O, Sr, Nd and Pb isotope geochemistry of MORB: Chemical Geology, v. 62, p. 157-176.

Johnson, D. M. H., P.R.; Conrey, R.M., 1999, XRF Analysis of Rocks and Minerals for Major and Trace Elements on a Single Low Dilution Li-tetraborate Fused Bead: Pullman, WA, JCPDS-International Centre for Diffraction Data, p. 843-867.

Knaack, C. C., Scott; Hooper, Peter, 1994, Trace Element Analyses of Rocks and Minerals by ICP-MS: Pullman, WA, WSU GeoAnalytical Laboratory, p. 1-18.

Lavecchia, G., 1987, The Tyrrhenian-Apennines system: structural setting and seismotectogenesis.: Tectonophysics, v. 147, p. 263-296.

Lavecchia, G. S., Francesco, 1990, The Tyrrhenian zone: a case of lithosphere extension control of intra-continental magmatism.: Earth and Planetary Science Letters, v. 99, p. 336-350.

Lavecchia, 1996, The tectonic significance of Italian magmatism: an alternative view to the popular interpretation.: Terra Nova, v. 8, p. 435-446.

Lux, D. R., 2003, Reading the Plagioclase Record, *in* GSA Northeastern Section - 38th Annual Meeting, Maine.

Othman, D. B. W., William M.; Patchett, Jonathan, 1989, The geochemistry of marine sediments, island arc magma genesis, and crust-mantle recycling.: Earth and Planetary Science Letters, v. 94, p. 1-21.

Perini, G. C., Sandro; Francalanci, Lorella; Davidson, Jon P., 2000, The relationship between potassic and calc-alkaline post-orogenic magmatism at Vico volcano, central Italy.: Journal of Volcanology and Geothermal Research, v. 95, p. 247-272.

Poli, G. F., Frederick A.; Ferrara, Giorgi, 1984, Geochemical characteristics of the South Tuscany (Italy) volcanic province: constraints on lava petrogenesis.: Chemical Geology, v. 43, p. 203-221.

Rollinson, H., 1993, Using Geochemical Data: Evaluation, Presentation, Interpretation, Longman Geochemistry Series: London, Prentice Hall, 352 p.

Stoppa, F., 2003, Epsilon strontium versus neodymium for eastern Italian volcanoes., *in* James, K., ed.: Chieti, Italy.

Van Bergen, M. J., 1985, Common trace-element characteristics of crustal- and mantle-derived K-rich magmas at Mt. Amiata (central Italy). Chemical Geology, v. 48, p. 125-135.

Van Bergen, M. J. G., Claudio; Ricci, Carlo Alberto, 1983, Minette inclusions in the rhyodacitic lavas of Mt. Amiata (central Italy): mineralogical and chemical evidence of mixing between Tuscan and Roman type magmas.: Journal of Volcanology and Geothermal Research, v. 19, p. 1-35.

Vollmer, R. H., C.J., 1980, Lead isotopic composition of the potassic rocks from Roccamonfina (South Italy). Earth and Planetary Science Letters, v. 47, p. 91-101.

Volpi, G. M., Adele; Fiordelisi, Adolfo, 2003, Investigation of geothermal structures by magnetotellurics (MT): an example from the Mt. Amiata area, Italy.: Geothermics, v. 32, p. 131-145.

Table 1: Major element wt.% for Amiata rock suite.

	SiO_2	TiO_2	Al_2O_3	FeO	MnO	MgO	CaO	Na_2O	K_2O	P_2O_5
KEJ-1	66.89	0.516	16.31	3.37	0.061	1.54	2.64	2.31	6.19	0.170
KEJ-2	66.78	0.543	16.56	3.33	0.058	1.44	2.80	2.33	5.98	0.169
KEJ-4	66.52	0.525	16.59	3.56	0.063	1.48	3.10	2.37	5.62	0.179
KEJ-7	65.12	0.567	17.78	3.70	0.065	1.63	2.87	2.19	5.88	0.185
KEJ-9	65.66	0.613	16.90	3.97	0.070	1.78	3.05	2.22	5.54	0.197
KEJ-12	65.98	0.539	16.94	3.53	0.062	1.53	2.94	2.29	6.01	0.181
KEJ-13	65.86	0.566	16.71	3.85	0.069	1.67	2.99	2.28	5.82	0.184
KEJ-14	66.26	0.554	17.05	3.56	0.062	1.49	2.64	2.25	5.96	0.173
KEJ-15	67.43	0.518	15.86	3.33	0.060	1.34	3.00	2.28	6.01	0.164
KEJ-17	66.31	0.536	16.34	3.48	0.062	1.58	3.06	2.32	6.13	0.182
KEJ-19	62.06	0.677	17.47	4.70	0.081	2.73	4.50	1.98	5.55	0.243
KEJ-21	66.93	0.529	16.17	3.66	0.065	1.54	2.87	2.29	5.78	0.171

Table 2: Trace element concentrations for the Amiata suite of trachydacites

	KEJ-1	KEJ-2	KEJ-4	KEJ-7	KEJ-9	KEJ-12	KEJ-13	KEJ-14	KEJ-15	KEJ-17	KEJ-19	KEJ-21
La	74.27	72.69	74.68	73.50	69.92	69.97	73.71	70.73	74.79	67.06	83.80	73.04
Ce	142.86	135.40	138.67	143.72	135.77	131.74	139.57	133.64	138.64	126.71	136.85	138.91
Pr	15.67	15.23	15.39	15.19	14.45	14.39	15.88	14.91	15.11	13.77	17.11	15.33
Nd	57.66	56.08	56.61	56.14	53.37	53.61	58.83	54.97	55.38	51.22	63.76	56.79
Sm	11.08	11.11	11.08	10.98	10.73	10.40	11.43	10.85	10.64	10.04	12.61	10.96
Eu	1.64	1.50	1.42	1.74	1.38	1.55	1.66	1.49	1.45	1.51	1.83	1.44
Gd	7.82	7.96	7.85	7.93	7.63	7.50	8.27	7.80	7.76	7.24	9.24	8.06
Tb	1.12	1.13	1.13	1.16	1.11	1.08	1.19	1.14	1.13	1.04	1.30	1.17
Dy	6.00	6.17	6.15	6.34	6.09	5.95	6.54	6.31	6.16	5.73	6.99	6.44
Ho	1.16	1.18	1.16	1.19	1.15	1.14	1.22	1.18	1.14	1.09	1.31	1.23
Er	2.99	3.11	3.03	3.07	3.03	2.97	3.18	3.07	3.05	2.87	3.33	3.19
Tm	0.43	0.45	0.44	0.46	0.45	0.42	0.47	0.45	0.44	0.41	0.47	0.47
Yb	2.69	2.75	2.70	2.83	2.79	2.57	2.82	2.78	2.63	2.50	2.90	2.84
Lu	0.41	0.42	0.42	0.42	0.43	0.40	0.43	0.42	0.40	0.39	0.46	0.43
Ba	650	553	486	676	431	631	582	572	512	615	627	491
Th	41.4	42.9	43.8	45.6	49.8	42.5	42.1	44.9	43.9	42.0	46.9	46.2
Nb	16.69	17.26	17.57	18.45	20.00	17.46	17.82	18.02	17.33	16.61	19.03	18.00
Y	29.28	30.32	31.17	31.71	28.91	30.40	32.52	31.70	31.84	29.57	36.35	33.64
Hf	6.75	6.75	7.44	7.52	7.76	7.17	7.21	7.36	6.97	6.58	7.98	7.09
Ta	1.50	1.84	1.56	1.61	1.72	5.63	1.52	1.90	1.52	1.49	1.92	1.61
U	10.07	10.67	10.45	10.46	11.40	10.25	10.17	10.93	10.63	10.09	11.24	11.39
Pb	59.54	59.07	57.83	63.24	59.37	60.19	60.12	61.47	58.70	58.95	62.09	59.95
Rb	356	348	351	308	310	350	339	358	377	364	322	382
Cs	44.60	43.23	45.22	34.59	20.89	40.85	37.84	41.53	45.20	40.96	34.68	45.58
Sr	348	336	357	422	327	385	379	353	372	387	433	354
Sc	10.3	10.4	11.1	11.6	12.7	11.4	12.0	11.3	10.7	11.2	17.0	11.6
Zr	215	214	242	246	251	236	237	246	230	220	271	234

Table 3: Stable Isotope (Sr, Rb, and Pb) ratios for the Amiata suite

	$^{87}Sr/^{86}Sr$	$^{144}Nd/^{143}Nd$	$^{206}Pb/^{204}Pb$	$^{207}Pb/^{204}Pb$
KEJ-1		0.512105	18.8696	15.8394
KEJ-2	0.713068	0.512108	18.7415	15.7155
KEJ-4	0.713018	0.512094	18.7125	15.6758
KEJ-7	0.712925	0.512114	19.0882	16.2330
KEJ-9	0.712570	0.512137	18.9058	15.9656
KEJ-12	0.713024	0.512153	19.0066	16.0198
KEJ-13	0.712999	0.512203	18.7545	15.6774
KEJ-14	0.713025	0.512158	18.7092	15.6694
KEJ-15	0.713002	0.512113	18.7148	15.6767
KEJ-17	0.712859	0.512136	18.8234	15.7890
KEJ-19	0.712447	0.512147		
KEJ-21		0.512129	18.7295	15.6947

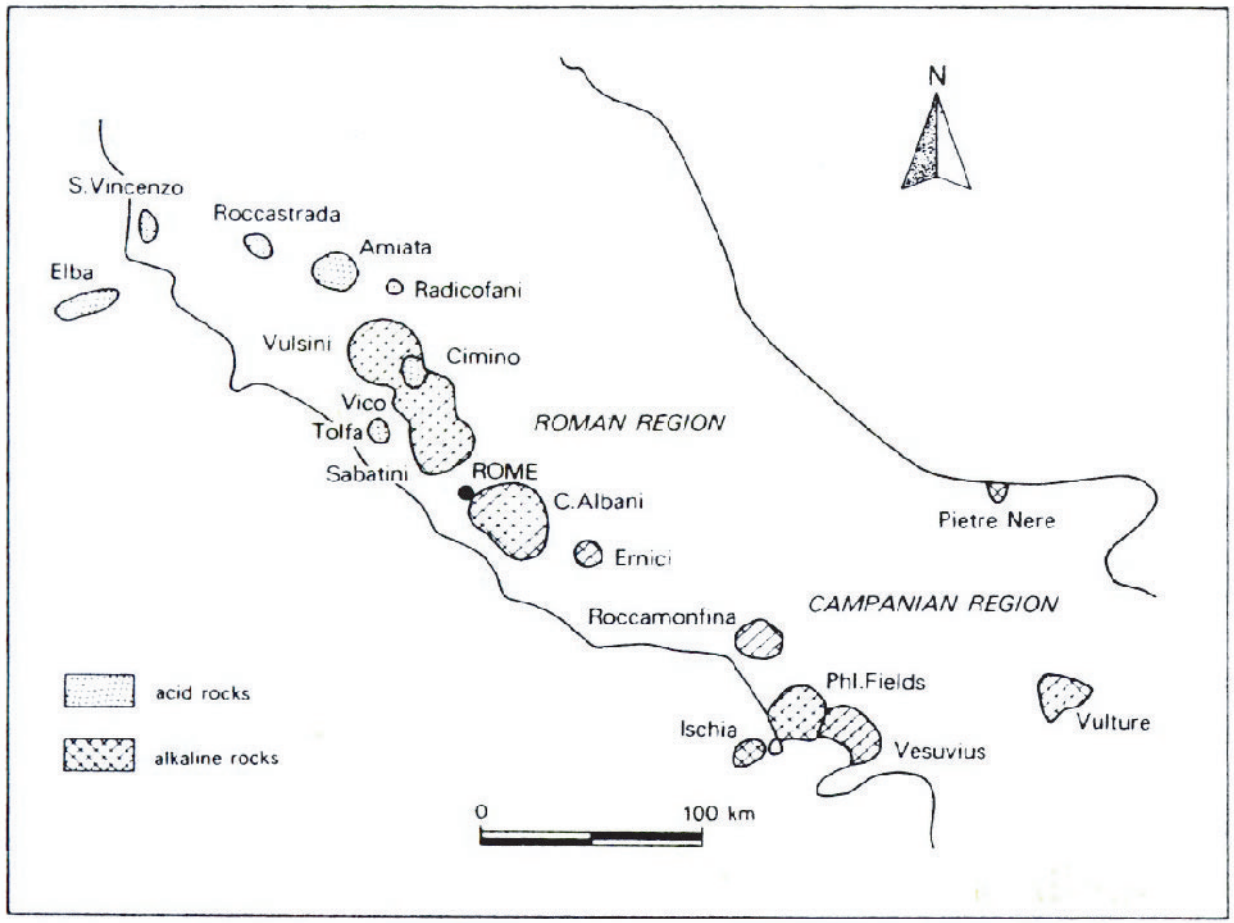

Figure 1: Location map showing the volcanoes of the TMP and RMP (alkaline vs. acid volcanics). Map taken from (Van Bergen, 1983).

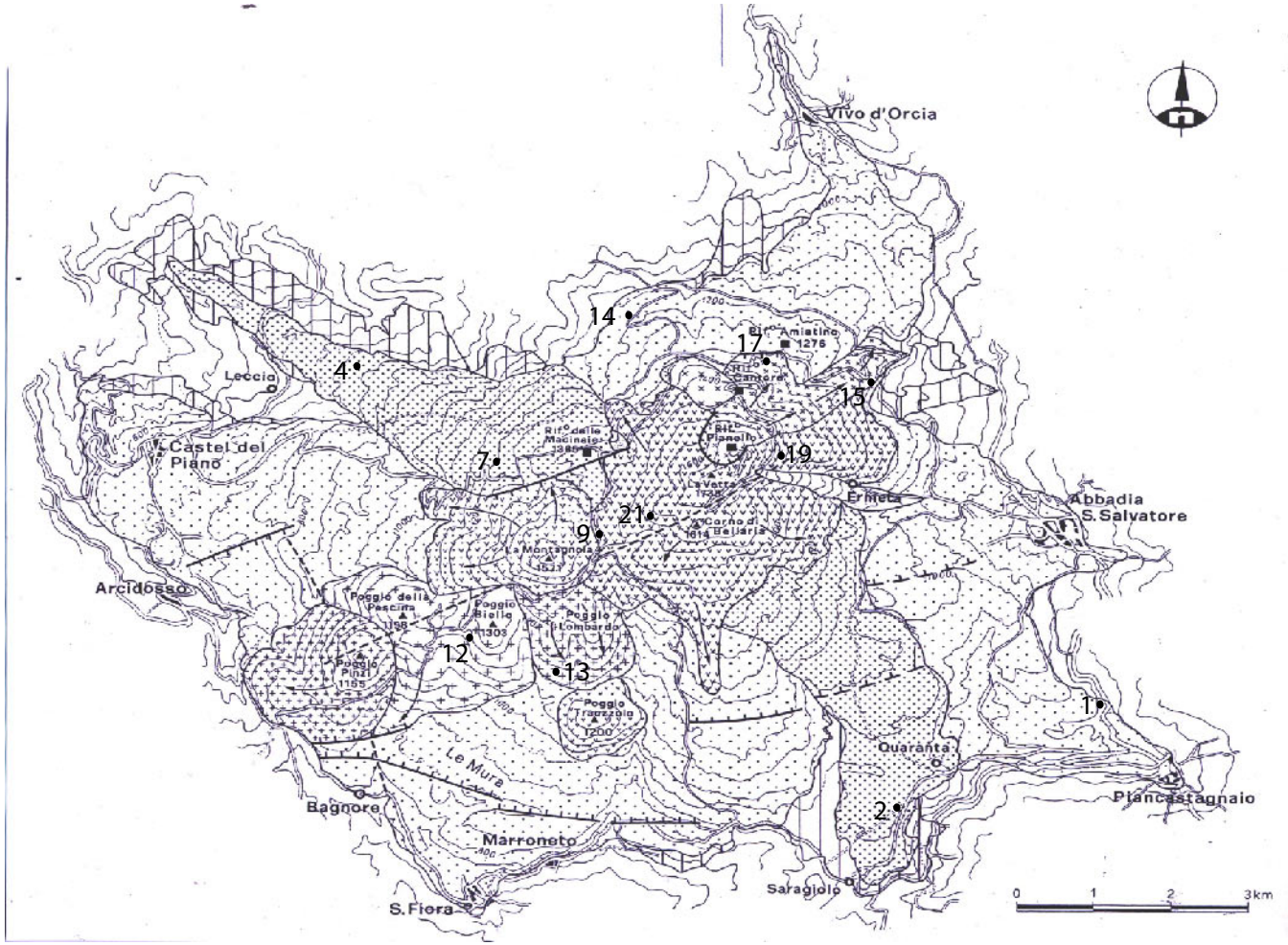

Figure 2: Site map showing locations of samples. Map taken from (Ferrari, 1996). Sites added by author.

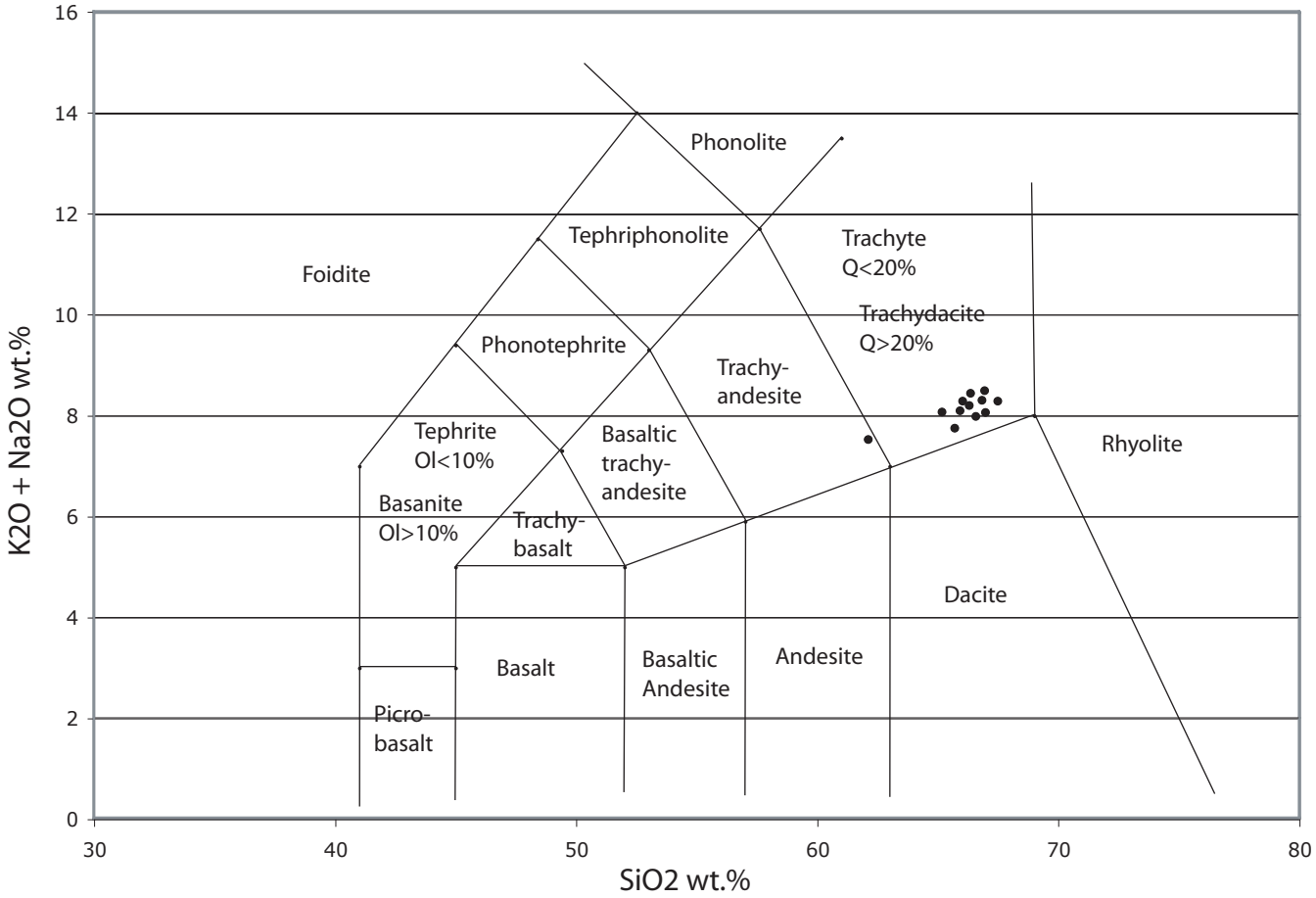

Figure 3: TAS (Total Alkali versus Silica) diagram for the Monte Amiata rock suite. Values for field taken from (Rollinson, 1993).

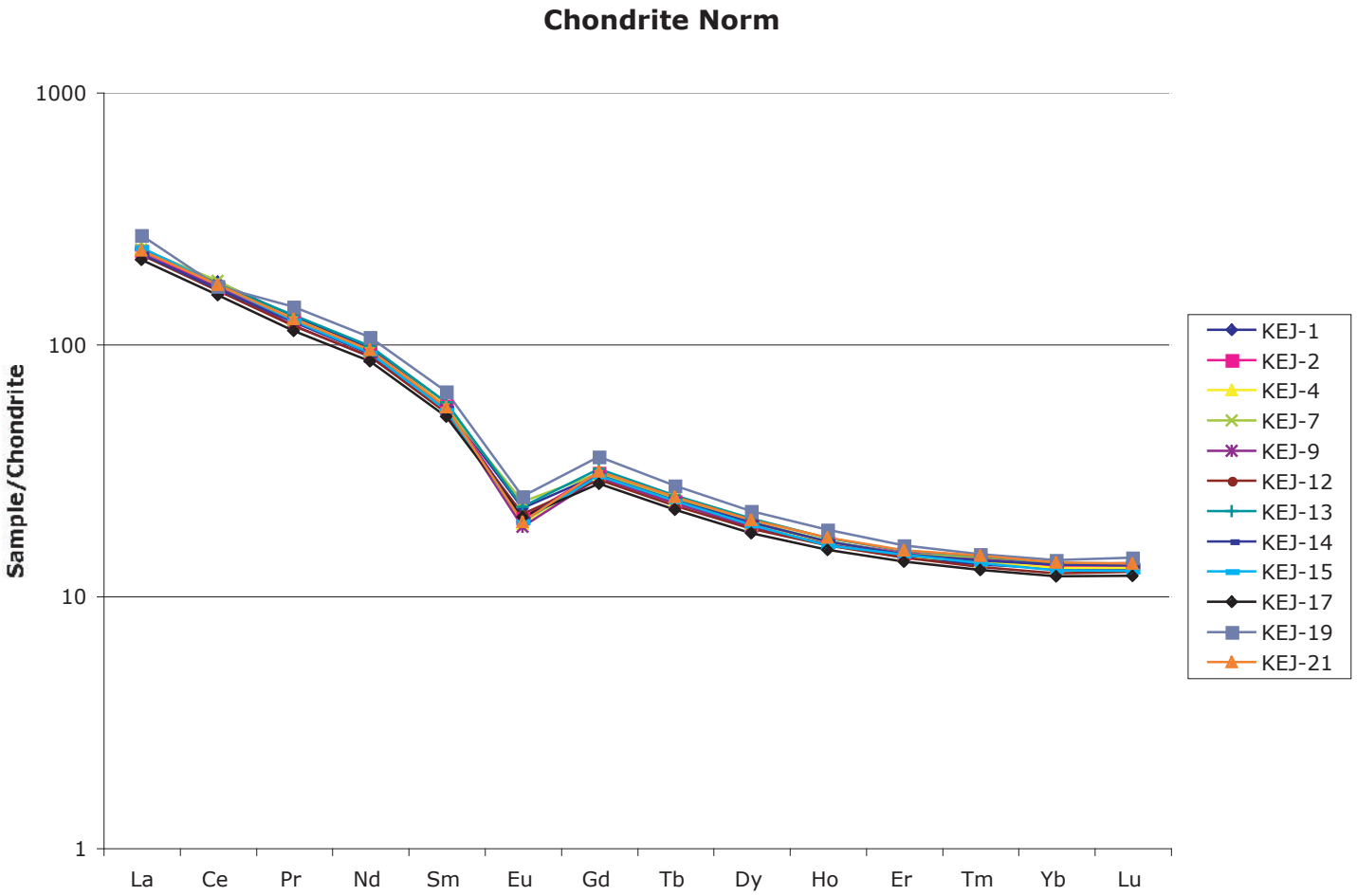

Figure 4: Chondrite normalized REEs. Chondrite normalization values taken from (Rollinson, 1993).

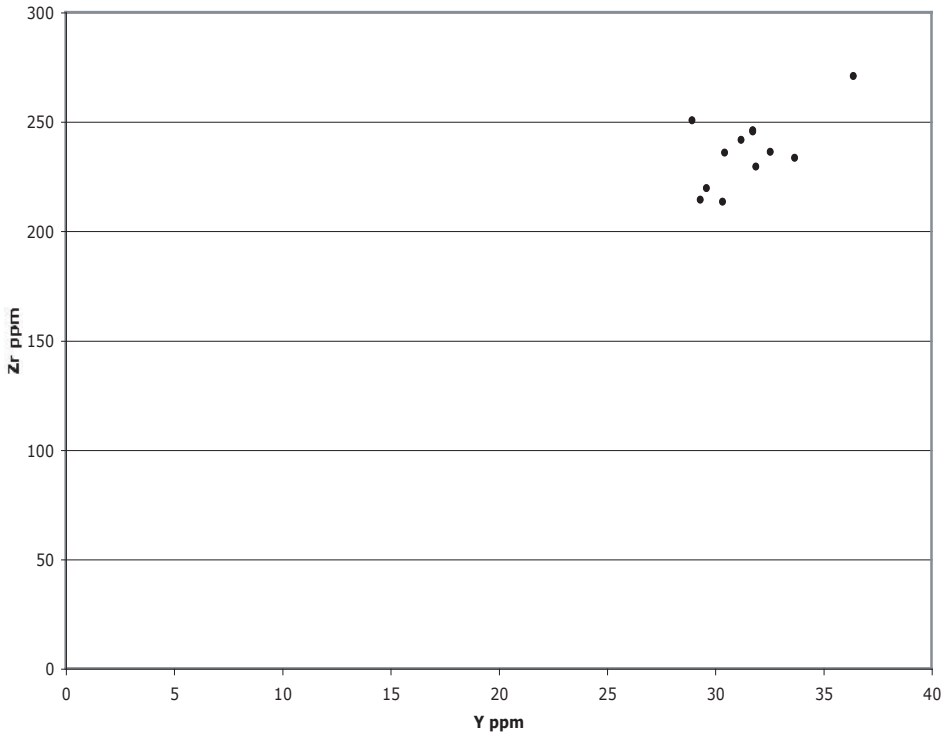

Figure 5a: Y vs. Zr plotted for Amiata rock suite.

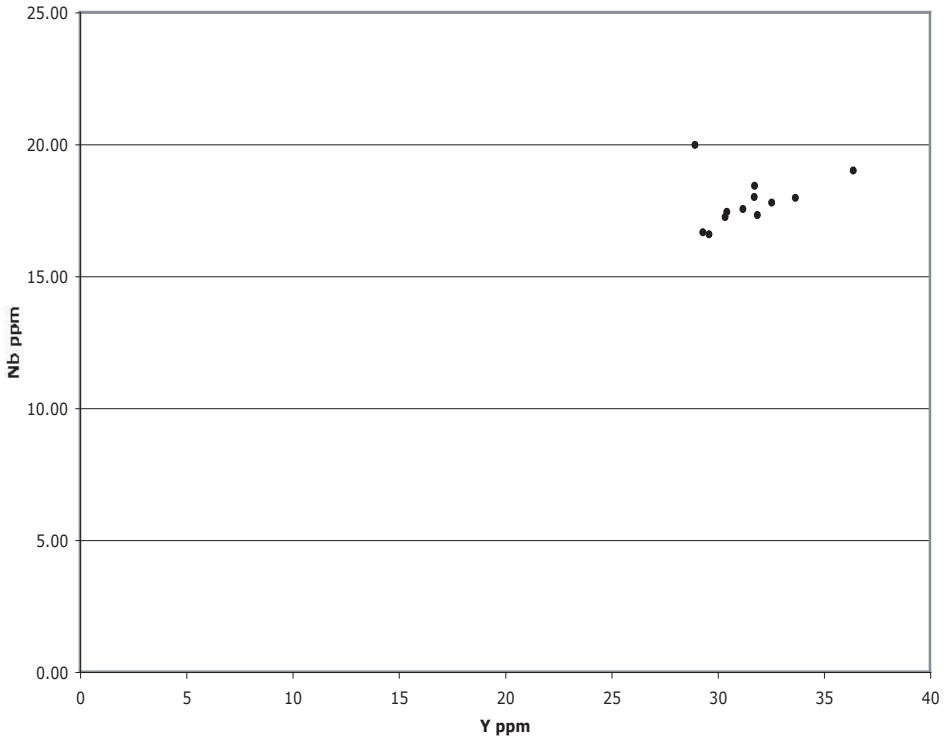

Figure 5b: Y vs. Nb plotted for Amiata rock suite.

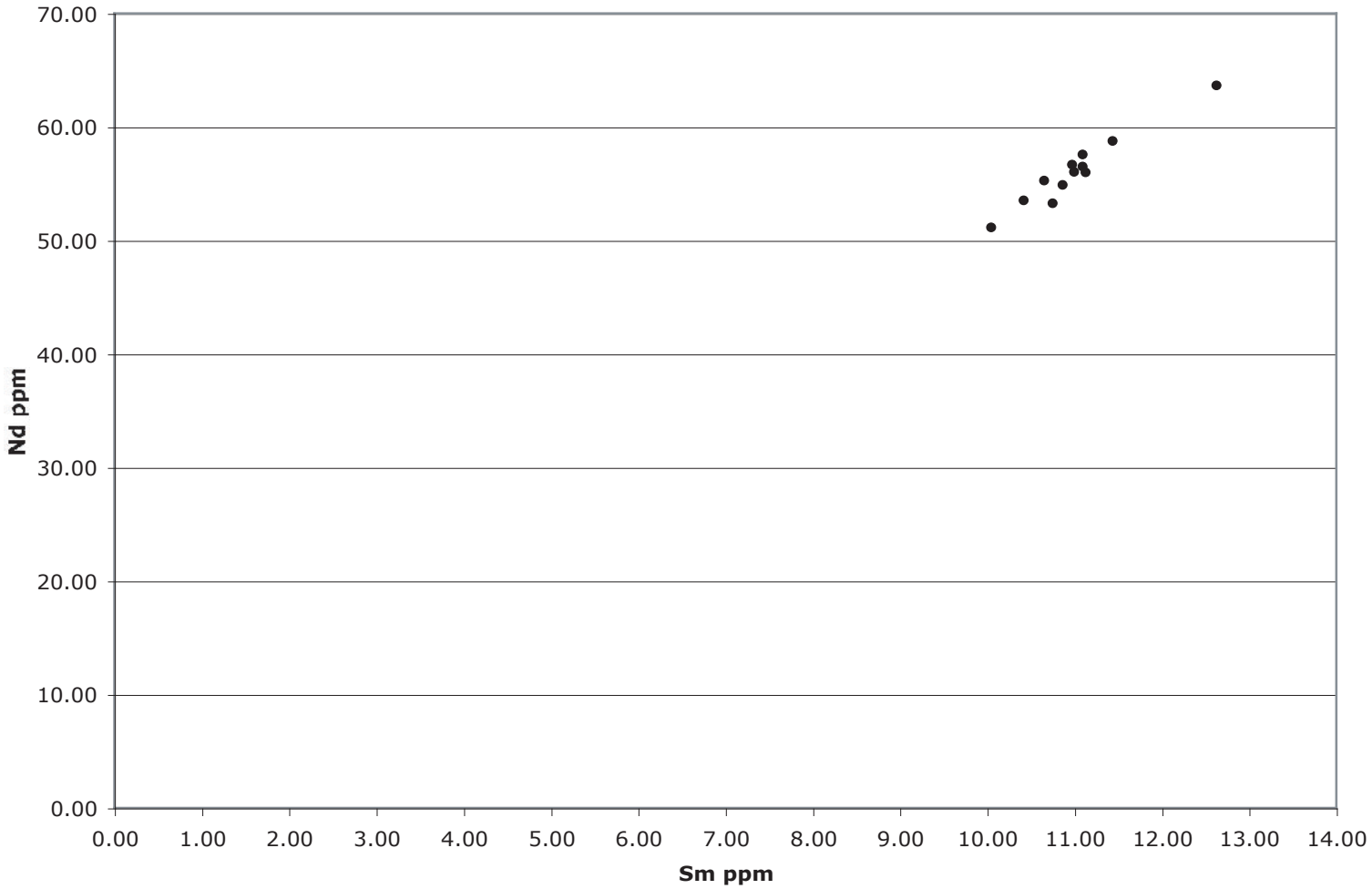

Figure 6: Nd concentrations plotted against Sm concentrations.

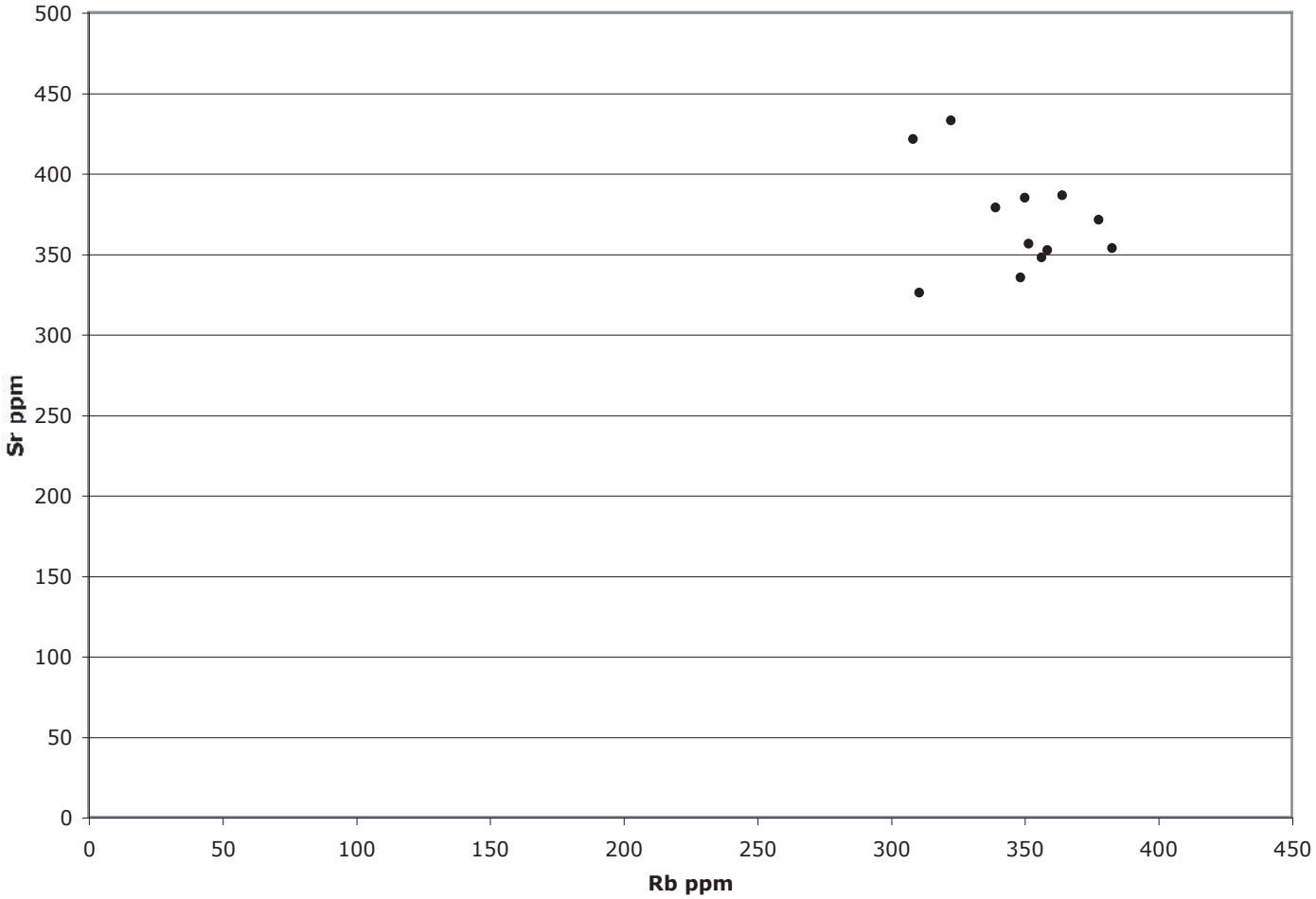

Figure 7: Sr concentrations versus Rb concentrations.

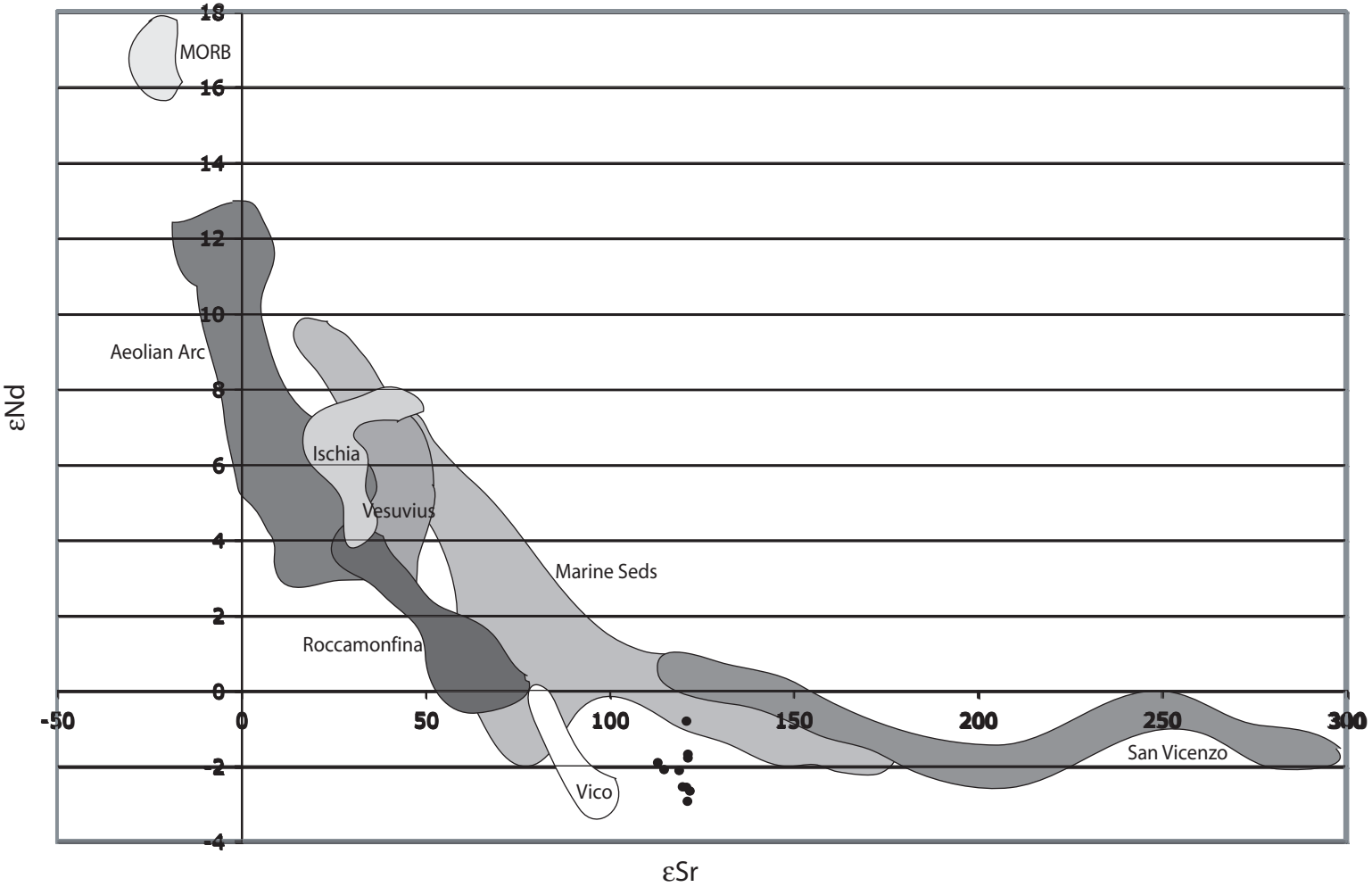

Figure 8: εSr plotted against εNd. Data used to make fields taken from (Caprarelli, 1993; Civetta, 1991; Conticelli, 1991; Conticelli, 1997; Ellam, 1989; Esperanca, 1992; Ferrara, 1989; Francalanci, 1993; Hawkesworth, 1979; Holm, 1982; Ito, 1987; Othman, 1989; Perini, 2000; Vollmer, 1980)

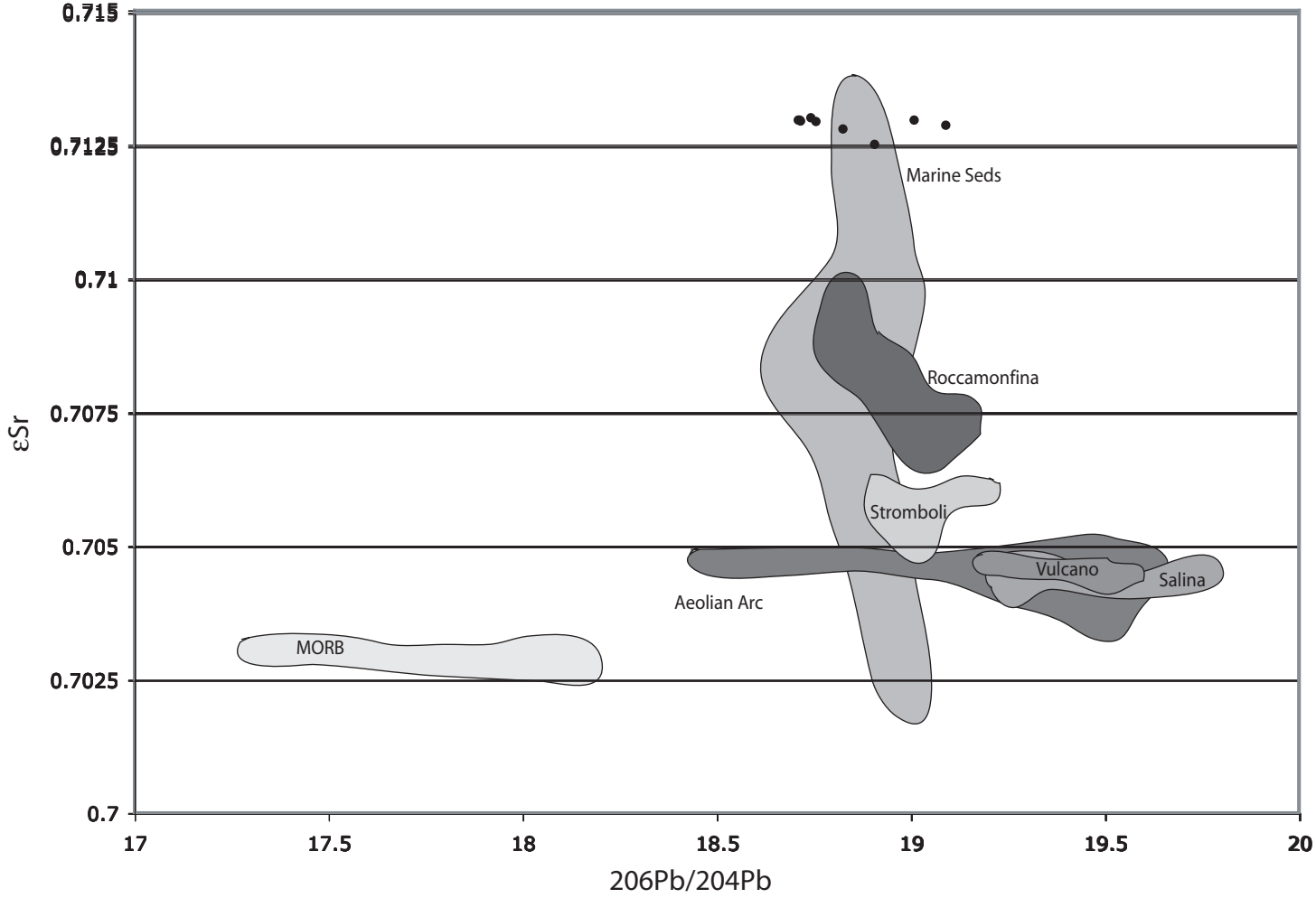

Figure 9: εSr plotted against the 206Pb/204Pb values. Data for fields taken from (Ellam, 1989; Esperanca, 1992; Francalanci, 1993; Hawkesworth, 1979; Ito, 1987; Othman, 1989; Vollmer, 1980)

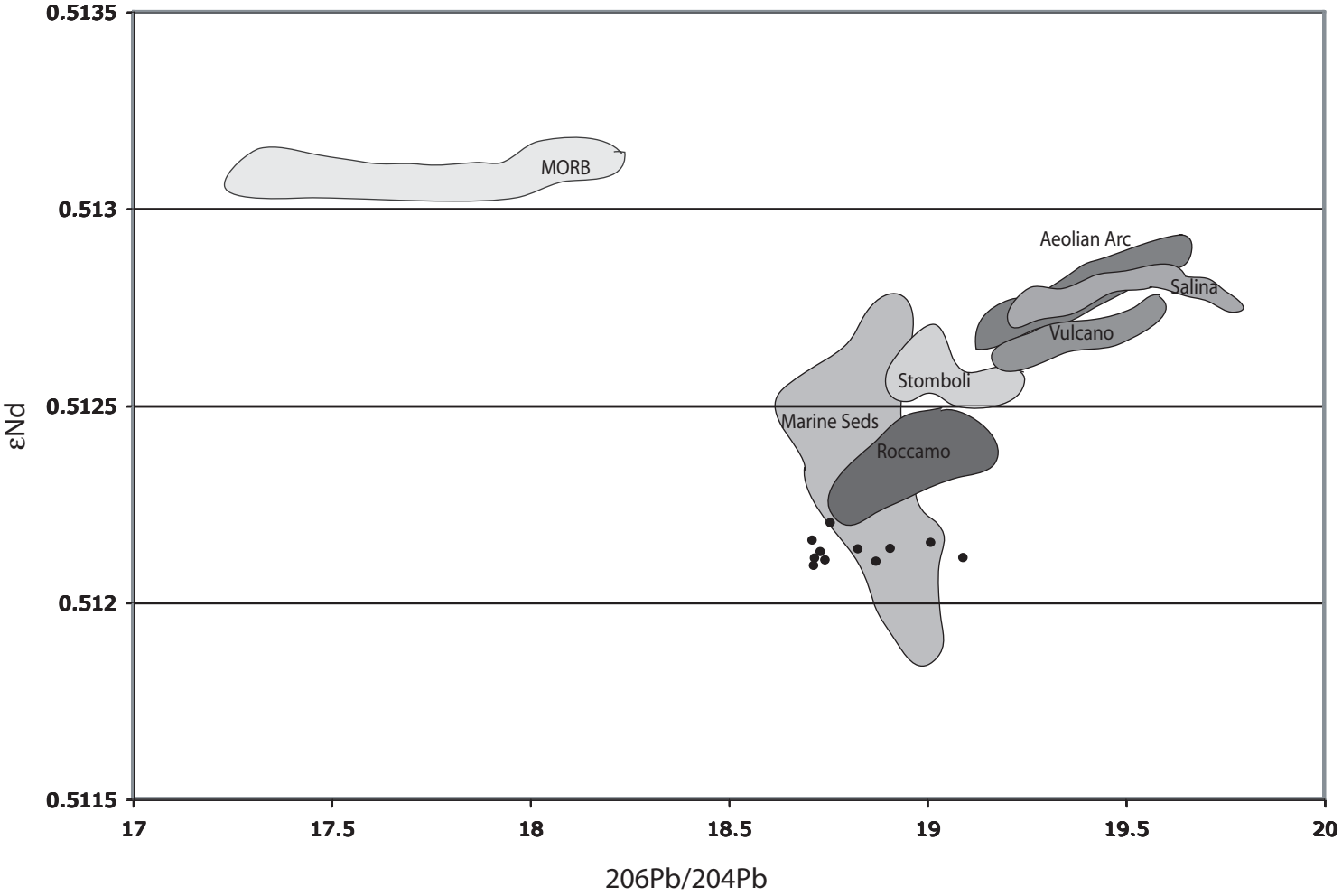

Figure 10: εNd versus 206Pb/204Pb for the Monte Amiata volcanics. Data for fields taken from (Ellam, 1989; Esperanca, 1992; Francalanci, 1993; Hawkesworth, 1979; Ito, 1987; Othman, 1989; Vollmer, 1980)

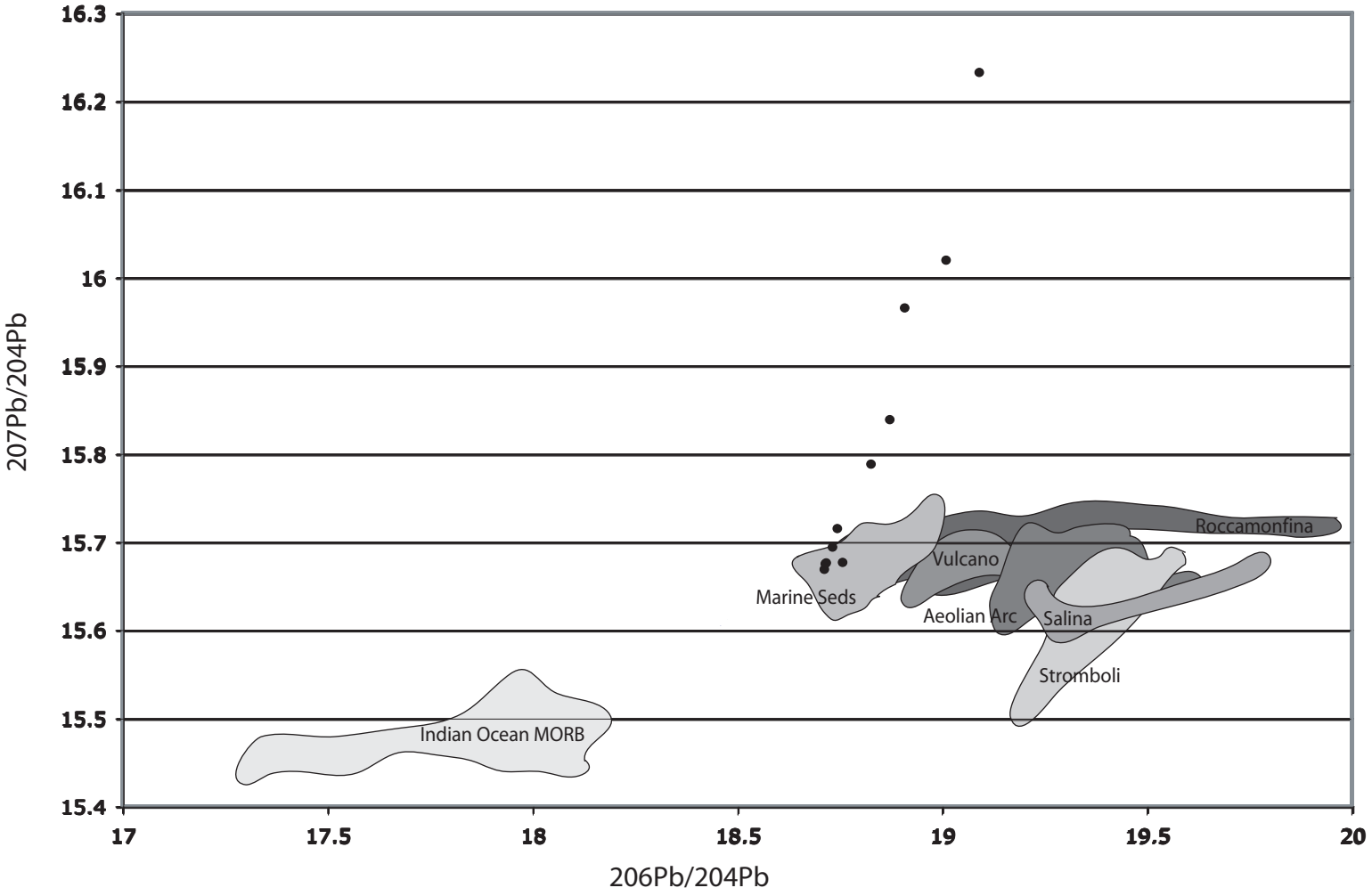

Figure 11: 207Pb/204Pb versus 206Pb/204Pb for the Amiata suite of rocks. Data for fields taken from (Ellam, 1989; Esperanca, 1992; Francalanci, 1993; Hawkesworth, 1979; Ito, 1987; Othman, 1989; Vollmer, 1980)